Available online at www.sciencedirect.com
SCIENCE DIRECT®
Biochemical and Biophysical Research Communications 329 (2005) 168–176
BBRC
www.elsevier.com/locate/ybbrc

Engineering and characterization of a divalent single-chain Fv angiotensin II fusion construct of the monoclonal antibody CC49 ☆,☆☆

Uwe A. Wittel [a], Maneesh Jain [a], Apollina Goel [a], Janina Baranowska-Kortylewicz [b], Takashi Kurizaki [b], Subhash C. Chauhan [a], Devendra K. Agrawal [d], David Colcher [e], Surinder K. Batra [a,c,*]

[a] Department of Biochemistry and Molecular Biology, University of Nebraska Medical Center, Omaha, NE 68198, USA
[b] Department of Radiation Oncology, University of Nebraska Medical Center, Omaha, NE 68198, USA
[c] Eppley Institute for Research in Cancer and Allied Diseases, University of Nebraska Medical Center, Omaha, NE 68198, USA
[d] Creighton University School of Medicine, Omaha, NE 68178, USA
[e] Department of Radioimmunotherapy, Beckman Research Institute at City of Hope National Medical Center, Duarte, CA, USA

Received 10 January 2005

Abstract

For the therapy of solid tumors, co-administration of angiotensin II (AngII) results in an increased uptake of drugs into the tumor interstitium. We have engineered a dimeric sc(Fv)$_2$-AngII fusion construct that combines the superior kinetics of covalent dimeric scFvs [sc(Fv)$_2$], recognizing the pancarcinoma tumor-associated antigen 72 (TAG-72), with the advantageous intrinsic activity of AngII. The binding characteristics of the fusion construct were unaltered by the addition of the AngII sequence [affinity constant K_A 1.18×10^7 and 8.42×10^6 M^{-1} for sc(Fv)$_2$ and sc(Fv)$_2$-AngII, respectively]. The binding of the fusion construct to the angiotensin receptor (AT_1) was similar to AngII, and the arterial contraction was $16 \pm 1\%$ of the response observed with norepinephrine. In animal studies, the radiolabeled sc(Fv)$_2$-AngII construct exhibited similar uptake and a more homogeneous distribution within the tumor as compared to sc(Fv)$_2$.

Keywords: Antibody engineering; scFv; Fusion protein; Angiotensin II; Cancer therapy; Radioimmunotherapy

For the treatment of hematological malignancies, monoclonal antibodies are promising new therapeutics that show good results, even in advanced stages of cancer [1]. The clinical success of antibody-based therapeutic regimens in solid tumors, however, did not live up to their initial promise [2]. While tumor cells of hematological malignancies typically are more easily accessible to the therapeutic antibody, the tumor cells in solid tumors are well "protected" by the solid stroma and poor vascularization [3]. For clinical therapy of solid tumors, a fast uptake of the antibody in the tumor interstitium is required. Unfortunately, this uptake relies almost exclusively on convection that is driven by pressure gradients between the interstitial fluid pressure (IFP) and the microvascular pressure (MVP) [4]. In solid tumors however, this pressure gradient is decreased [5,6]. The leaky

☆ This study was supported, in part, by a grant from the National Institutes of Health to J.B. (P50 CA72712) and the US Department of Energy (DE-FG02-95ER62024) to S.K.B.
☆☆ *Abbreviations:* IFP, interstitial fluid pressure; MVP, microvascular pressure; AngII, angiotensin II; scFv, variable single chain fragment; AT1, angiotensin receptor subtype 1; IMAC, immobilized metal affinity chromatography; NE, norepinephrine; %ID/g, percent injected dose per gram.
* Corresponding author. Fax: +1 402 559 6650.
E-mail address: sbatra@unmc.edu (S.K. Batra).

0006-291X/$ - see front matter © 2005 Elsevier Inc. All rights reserved.
doi:10.1016/j.bbrc.2005.01.101

nature of tumor vasculature, due to structural and functional abnormalities, and the absence of functional lymphatic system in tumor result in the decreased MVP and increased IFP [7–10]. This phenomenon leads to lowering or complete elimination of pressure gradients, thus impairing the macromolecular transport in the tumor [11,12].

For increasing the uptake of macromolecules into the tumor interstitium, an increase of the pressure gradient between the MVP and IFP can be achieved by the application of vasoactive drugs [13]. These drugs induce an increase in the systemic or local blood pressure that consequently elevates the MVP. Co-administration of angiotensin II (Ang II) is an attractive approach for enhancing the tumor uptake of macromolecules [14], since neoplastic blood vessels are devoid of smooth muscles and therefore lack the ability vascular contraction [15]. The administration of AngII results in increased tumor blood flow by diverting the blood flow from normal tissue, with contracted blood vessels, into the tumor, with neoplastic blood vessels incapable of contraction [16–18]. This phenomenon is believed to underlie the beneficial effect of angiotensin II combination therapies in the clinical, as well as experimental, settings [19–25]. In chemotherapeutic regimes, for example, the co-administration of angiotensin II, in the majority of the studies, led to an increased drug uptake in the tumor, thereby resulting in a positive effect on tumor therapy [26]. In radioimmunotherapy, however, the increase in antibody uptake in the tumor due to angiotensin II varied between different types of tumors [27,28].

The discrepancy between the clinical success of combinations of chemotherapy or microspheres with angiotensin II and the inconsistent observations with protocols involving antibodies can be explained on the basis of molecular size of the therapeutic molecules. With their molecular size of 150 K_d, IgGs are several-fold larger than chemotherapeutic drugs, however, IgGs still require diffusion into the interstitium of the tumor. On the other hand, micro spheres exceed the molecular weight of IgG, but these drugs are designed to embolize the vascular bed [29,30]. In that context, one reason for IgGs to stand behind chemotherapeutic drugs in angiotensin II combination treatments could be the slow pharmacological kinetics of IgGs that are closely related to the molecular weight of the molecule. Therefore, a combination of angiotensin II with small molecular weight antibody fragments, like diabodies, and single-chain Fvs (scFvs), with a higher ability for diffusion, could show a beneficial effect. This might be especially true since these molecules have shown excellent antigen binding properties in the past and led to a high tumor uptake with low distributions to normal tissues [31,32].

We have previously developed mono-, di-, and tetravalent scFvs directed against the pancarcinoma antigen TAG-72 [33–36]. These scFvs, especially as covalent dimeric and non-covalent tetrameric forms, exhibited excellent antigen binding and tumor uptake, and also showed outstanding pharmacological properties in preclinical studies [34]. Therefore, in the present study, we have combined the superiority of scFvs with the positive effects of angiotensin II in a genetically engineered fusion construct. The scFv-angiotensin fusion protein [sc$(Fv)_2$-AngII] was expressed as a soluble protein and purified by affinity chromatography. Further, binding of sc$(Fv)_2$-AngII to antigen (TAG-72) and angiotensin type1 receptor (AT_1) was characterized. We have also studied the in vivo bio-distribution of the fusion construct in tumor-bearing mice.

Materials and methods

Construction of the expression vector. As described previously, the divalent single-chain Fv [sc$(Fv)_2$:V_L-linker-V_H-linker-V_L-linker-V_H] was constructed by PCR amplification of the variable regions of the murine mAB CC49 and the 205C linker [32]. This construct served as template DNA for engineering of the His_6-sc$(Fv)_2$-AngII construct. The angiotensin construct was engineered by PCR using the forward primer P1, encoding for the hexahistidine tag (HisTag), and the reverse primer P2, encoding for a five amino acid spacer with the amino acid sequence Gly-Ser-Gly-Ala-Ala, and the eight amino acid sequence of angiotensin II Asp-Arg-Val-Tyr-Ile-His-Pro-Phe (Table 1).

The PCR product was ligated with *Eco*RI/*Not*I, purified, and independently ligated into the *Pichia pastoris* expression vector pPICZαA (Invitrogen, Carlsbad, CA, USA). The ligation mixtures were used to transform *Escherichia coli* OneShot TOP10F' competent cells (Invitrogen, Carlsbad, CA, USA), which were selected on low salt LB plates, containing 25 μg/ml zeocin. After restriction analysis and sequencing of the plasmid DNA, competent *P. pastoris* cells were transformed with *Sac*I-linearized constructs using the Pichia Easy-Comp kit according to the supplier's instructions (Invitrogen, Carlsbad, CA, USA). The cells were then selected on YPDS plates with 100 μg/ml zeocin and eight clones were cultured in induction medium to analyze the expressed proteins. The protein from an up-scaled batch of the selected clone was purified by immobilized metal affinity chromatography (IMAC), using the chelating resin Ni^{2+}–nitrilotriacetic acid (NTA) Superflow (Quiagen, Valencia, CA, USA) with 50 mM

Table 1
PCR primer sequences used for engineering of the sc$(Fv)_2$-AngII construct

Forward primer (P1)	5′-GGGG*AATTC***CATCATCACCACCATCAT**GACATTGTGATGTCACAGTCTCCA-3′
Reverse primer (P2)	5′-GGGC**GGCCGC**TTATTAGAATGGATGAATATATACTCGGTC*AGCAGCTCCACTTCC*TGAGGAGACGGTGA CTGAGGTTCCTTGA-3′

The angiotensin II sequence is underlined, and the spacer sequence is shown in italics in P2. The sequence coding for the hexahistidine tag is shown in bold letters in P1. Furthermore, the *Eco*RI site is marked in italics and underlined in P1, and the *Not*I site is in bold and underlined in P2.

sodium phosphate, 300 mM NaCl buffer as the mobile phase. Bound protein was eluted with buffer containing 250 mM imidazole and further subjected to size exclusion chromatography using a Superdex 200 column (1.6 × 60 cm, Pharmacia, Uppsala, Sweden) to separate dimeric and tetrameric forms. The purified product was concentrated with a Centricon YM-10 centrifugal filter device (Millipore, Bedford, MA, USA) and stored at −70 °C until further analysis.

SDS–PAGE. The purity and integrity of the constructs was analyzed by SDS–PAGE. The electrophoresis was performed using a 10% acrylamide gel under reducing (5% β-mercaptoethanol) and non-reducing conditions. Gels were either stained by Coomassie blue, or in the case of ^{125}I-labeled constructs, directly exposed to film for autoradiography after drying.

Solid-phase competitive ELISA. The specific immuno-reactivity of the sc(Fv)$_2$-AngII and control constructs without angiotensin was assessed at various points in the purification process, as well as in the final purified product. As published previously [37], polystyrene plates were coated with 50 ng/well bovine submaxillary gland mucin (BSM) and dried overnight at 37 °C, followed by blocking with 5% bovine serum albumin (BSA) at 37 °C for 1 h. Serial dilutions of CC49 IgG and the constructs were prepared and 5 μl was added to 45 μl of 1% BSA in PBS containing 6 ng/ml biotinylated CC49 IgG. After 2 h at room temperature, the plates were incubated with alkaline phosphatase-conjugated streptavidin for 90 min, also at room temperature. After developing with *p*-nitrophenyl phosphate substrate, the absorption was assessed at 410 nm.

Surface plasmon resonance studies. The binding kinetics of the constructs were assessed by surface plasmon resonance detection using a BIAcore biosensor (Pharmacia Biosensor, Uppsala, Sweden) as described previously [35,38]. Briefly, BSM was immobilized on a CM5 dextran sensor chip in 100 mM sodium acetate, pH 3.0, by amine coupling (Amine Coupling Kit, Pharmacia, Uppsala, Sweden). The binding analysis was performed in HBS buffer (10 mM Hepes, pH 7.4, 0.15 M NaCl, 3.4 μM EDTA, and 0.005% surfactant P_2O) at a flow rate of 30 μl/min at 25 °C. The kinetic constants for association (K_A) were evaluated using the BIAevaluation 3.0.2 software package (BIAcore, Piscataway, NJ, USA).

Angiotensin II receptor binding assay. The affinity of the sc(Fv)$_2$-AngII fusion construct to the AT$_1$ receptor was determined by using commercially available cloned human angiotensin II receptor subtype 1, produced in CHO cells (NEN, Boston, MA). Binding of the fusion construct was determined by its ability to compete with angiotensin II analogue {(Sar$_1$,Ile$_8$)-angiotensin II [(Sar$_1$,Ile$_8$)-AngII]}. The binding assay was performed in polypropylene plates in 170 μl total volume according to the supplier's protocol. Briefly, a 500 μl aliquot of CHO cell membranes was diluted with 7 ml of incubation buffer (50 mM Tris–HCl, pH 7.4, 5 mM $MgCl_2$, 1 mM EDTA, and 0.1% BSA). ^{125}I-(Sar$_1$,Ile$_8$)-angII (specific activity >2200 Ci/mmol; 0.01 ml) was added to 150 μl of diluted membranes to produce a final concentration of a radio-ligand of 0.2 nM. For competitions, 10 μl cold (Sar$_1$,Ile$_8$)-AngII or sc(Fv)$_2$-AngII was added to a final concentration of 0–10 μM. The mixtures were incubated for 60 min at 37 °C. GF/C filters, presoaked with 0.3% polyethyleneimine in incubation buffer, were used to separate bound from free ligand. Filters were washed nine times with 200 μl ice-cold 50 mM Tris–HCl, pH 7.4, at 4 °C. The radioactivity of the washed filters was assessed with a Packard Minaxi AutoGamma 5000 γ-counter (Packard, Meriden, CT, USA).

Functional effect of the sc(Fv)$_2$-AngII fusion construct on blood vessels. The functional effect of sc(Fv)$_2$-AngII on rat aortic arteries was examined by a dose–response of the fusion construct and the sc(Fv)$_2$ in comparison to the functional effect with norepinephrine (NE). The aortic artery was removed from the rat following anesthesia in a CO_2 chamber. Three millimeter arterial rings were placed in modified Krebs solution (NaCl 115.5 mM, KCl 4.6 mM, NaH_2PO_4 1.16 mM, $MgSO_4$ 1.16 mM, $CaCl_2$ 2.5 mM, $NaHCO_3$ 21.9 mM, and glucose 11.1 mM at pH 7.4, aerated with 95% O_2/5% CO_2) and subjected to 1 g pre-load tension before being allowed to equilibrate at 37 °C for a minimum of 2 h.

Two responses to a maximal concentration of NE (5 μM) were obtained. After washing the tissue, a complete dose–response curve to NE, followed by a complete dose–response curve to sc(Fv)$_2$-AngII, was constructed by an approximately threefold stepwise increase of agonist after the response to the previous dose had reached a plateau. The data were calculated and plotted as the percent maximum response to NE.

^{125}I labeling and analysis of radiolabeled sc(Fv) constructs. The sc(Fv) constructs were labeled with Na^{125}I as described by Colcher et al. [39]. In a tube coated with 20 μg Iodo-Gen (Pierce, Rockford, IL USA), 100 μg protein in 0.1 M sodium phosphate buffer and 0.1 mCi Na^{125}I was mixed and incubated for three minutes at room temperature. The free iodine was separated from the labeled product by size exclusion chromatography over a Sephadex 25 column (Sigma, St. Louis, MO, USA).

Instant thin layer chromatography was performed with the purified, labeled product with 25% methanol in water as solvent to determine the percentage of bound ^{125}I. All radioactive products showed less than 5% free radioactivity.

HPLC analysis. The extent of aggregation and the degree of dimerization were monitored by HPLC gel-filtration. Samples were injected onto a TSK G2000 and TSK G3000 (Toso Haas, Tokyo, Japan) size exclusion column connected in a series with 67 mM phosphate and 100 mM KCl buffer (pH 6.8) as a mobile phase at a flow rate of 0.5 ml/min. The absorption was monitored at 280 nm and 0.25 ml fractions were collected [32]. The radioactivity of the fractions was determined as described above.

In vivo tumor localization and macro-autoradiography. All animal studies were performed in accordance with the US Public Health Service Guidelines for the Care and Use of Laboratory Animals and approved by the UNMC IACUC. The mice were held under standardized conditions with a 12/12 h dark/light cycle. LS-174T cells (4×10^6 cells per animal) were implanted subcutaneously in 6–8-week-old female athymic mice (nu/nu, Charles River, Wilmington, MA). Eight to 10 days later, when the tumor volume reached nearly 200–300 mm^3, animals were injected with ^{125}I-labeled constructs (0.37 MBq) via the tail vain (five animals per group). After four hours, the animals were sacrificed. Organs and blood were taken and the radioactivity was assessed as described above. After counting, the tumors were fixed in 10% phosphate-buffered formalin and embedded in paraffin. Sections (20 μm) of the tumors were cut, mounted on glass slides, and exposed to X-ray film for 14 days.

Statistical analysis. The statistical analyses were performed with GraphPad Prism 2.01 (GraphPad Software, San Diego, CA).

Results

Characterization and quality control of the protein preparation

The covalent dimeric scFv of CC49 linked to the octapeptide angiotensin II via a five amino acid spacer [sc(Fv)$_2$-AngII] and the covalent dimeric scFv of CC49 (Fig. 1) were secreted as soluble, active proteins by the transformed *P. pastoris*, 96–108 h after methanol induction. The two-step purification of the culture supernatant, first by Ni^{2+}–NTA affinity chromatography and imidazole elution, followed by size exclusion chromatography, yielded in both instances a covalent dimeric scFvs with greater than 90% purity (Fig. 2). HPLC analyses of both ^{125}I-labeled constructs indicated over 95% of the radioactivity in fractions associated with the molecular weight of the construct, thus suggesting that iodination does not alter the overall integrity of either of the con-

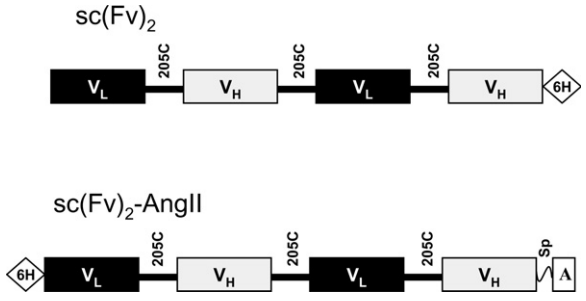

Fig. 1. Schematic presentation of the design of $sc(Fv)_2$ and $sc(Fv)_2$-AngII constructs. The variable regions of the light (V_L) and heavy chains (V_H) of MAb CC49 were connected with 205C linker to form a covalent dimeric $sc(Fv)_2$ with a C-terminal hexahistidine purification tag (6H). The $sc(Fv)_2$-AngII construct was engineered from $sc(Fv)_2$ by moving the hexahistidine tag to the N-terminal and tethering angiotensin II sequence (A) to the C-terminal of V_H through a 5 amino acid spacer (Sp).

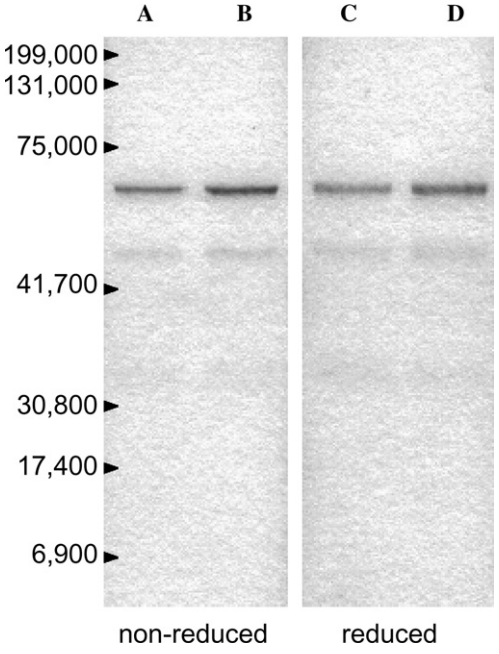

Fig. 2. The SDS–PAGE under non-denaturing (A,B) and denaturing (C,D) conditions, followed by Coomassie blue staining, shows more than 90% purity of the $sc(Fv)_2$ and $sc(Fv)_2$-AngII after IMAC and size fractionation. Both constructs appear as one band of approximately 60 kDa, the theoretical weight of the dimeric sc(Fv). (A) $sc(Fv)_2$-AngII, (B) $sc(Fv)_2$ without β-mercaptoethanol, (C) $sc(Fv)_2$-AngII, and (D) $sc(Fv)_2$ with β-mercaptoethanol.

structs (Fig. 3). The stability of the constructs during iodination was further observed in SDS–PAGE, where under denaturing and non-denaturing conditions the radiolabeled constructs were intact (data not shown).

Binding characteristics of the $sc(Fv)_2$ and $sc(Fv)_2$-AngII

Two changes possibly affecting the antigen binding were made to the previously reported dimeric $sc(Fv)_2$ described in Goel et al. [32]. The purification HisTag was

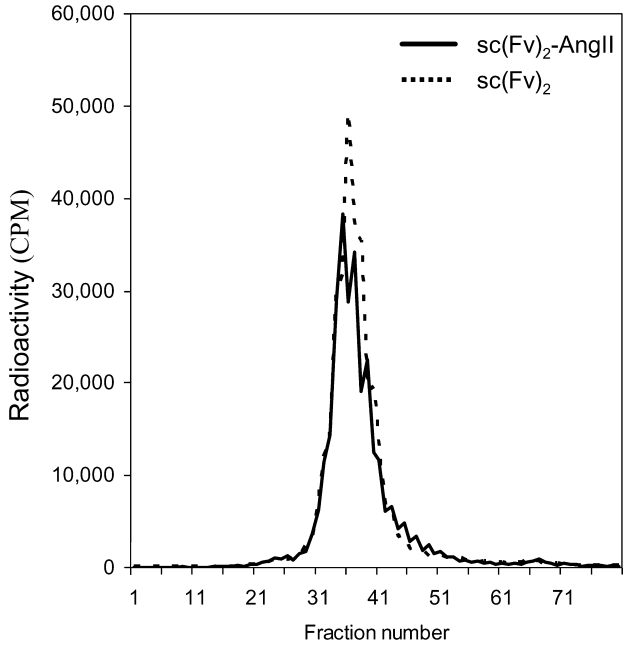

Fig. 3. The HPLC size fractionation of the radiolabeled scFv with a T-2000 and T-3000 column in series does not reveal any aggregates of the $sc(Fv)_2$-AngII or $sc(Fv)_2$ that might form during purification or ^{125}I labeling.

moved from the C-terminal end to the N-terminal end of the molecule and the spacer as well as the angiotensin II sequence was added to the C-terminal end of the $sc(Fv)_2$ (Fig. 1). The antigen binding was assessed by solid phase competitive ELISA to biotinylated CC49 IgG and by surface plasmon resonance studies.

When compared to the $sc(Fv)_2$, the ability to compete with whole IgG in solid phase competitive ELISA was not affected by the modifications to the $sc(Fv)_2$-AngII molecule. The concentration of the single-chain construct to reduce CC49 binding by 50% was determined to be 6.78×10^{-4} M for $sc(Fv)_2$-AngII and 5.26×10^{-4} M for $sc(Fv)_2$, respectively (Fig. 4). To assess the off rates as well as the real-time binding kinetics of both constructs, surface plasmon resonance studies were performed. As shown in Fig. 5, the profiles obtained in the BIAcore evaluation of both constructs were similar. The on rates (k_{on}) were unaltered by the changes in the $sc(Fv)_2$-AngII molecule and were determined to be 2.97×10^4 and 2.84×10^4 $(Ms)^{-1}$ for $sc(Fv)_2$-AngII and $sc(Fv)_2$, respectively. Furthermore, the modifications of the $sc(Fv)_2$ did not lead to an alteration of the off rate (k_{off}), the rate an antibody diffuses off from its target molecule. The individual values obtained for the off rates were 2.52×10^{-3} s^{-1} for the $sc(Fv)_2$-AngII and 3.38×10^{-3} s^{-1} for the $sc(Fv)_2$. Consequently, the calculation of the kinetic association constants K_A did not reveal differences in the binding affinities of these two constructs and led to values of 1.18×10^7 M for $sc(Fv)_2$-AngII and 8.42×10^6 M for $sc(Fv)_2$.

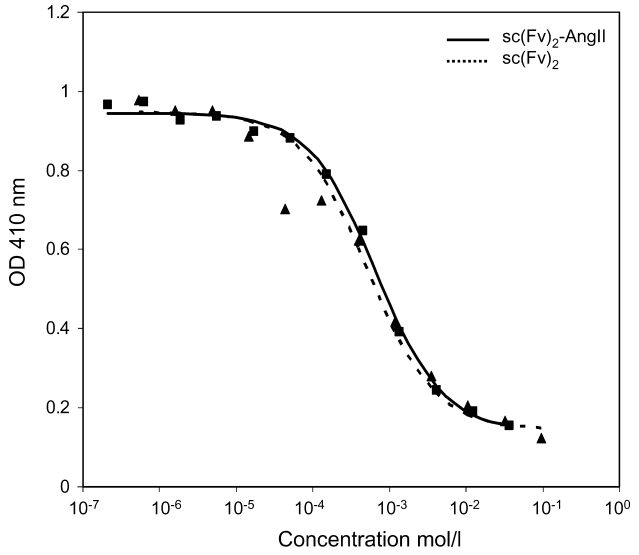

Fig. 4. Binding of $sc(Fv)_2$ (triangles) and $sc(Fv)_2$-AngII (squares) constructs with BSM (antigen). Increasing amounts of constructs were allowed to compete with biotinylated CC49 IgG for binding to BSM in a solid phase ELISA. A 50% inhibition of CC49-binding was achieved at approximately the same concentration of 6.78×10^{-4} M for $sc(Fv)_2$-AngII and 5.26×10^{-4} M for $sc(Fv)_2$, respectively, indicating their similar binding affinities of the two constructs to BSM.

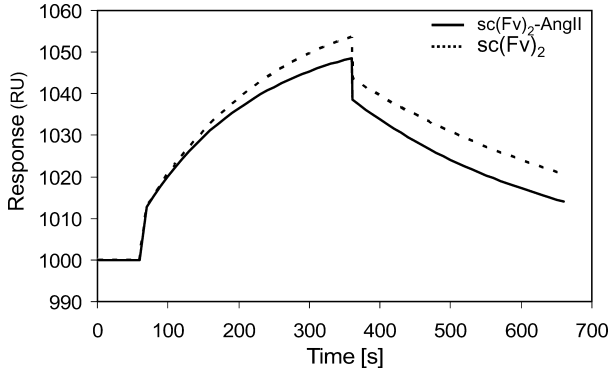

Fig. 5. Real-time binding kinetics of $sc(Fv)_2$ and $sc(Fv)_2$-AngII. The binding kinetics were analyzed by surface plasmon resonance to a BSM coated chip. The two constructs exhibited similar on and off rates, and thus had comparable association constants, indicating that the altered design of $sc(Fv)_2$ had no effect on the inherent specific binding of the $sc(Fv)_2$.

Angiotensin II receptor binding and functional effect

Binding of the angiotensin II peptide in the $sc(Fv)_2$-AngII fusion protein to its receptor was evaluated using a commercially available cloned human angiotensin II receptor subtype 1 produced in CHO cells with a no-carrier-added ^{125}I-(Sar_1,Ile_8)-AngII as a ligand. Non-radioactive-(Sar_1,Ile_8)-AngII (positive control) and $sc(Fv)_2$-AngII construct served as competitors. $Sc(Fv)_2$ CC49 was used as a negative control. The $sc(Fv)_2$-AngII fusion construct competed effectively with the ^{125}I-(Sar_1,Ile_8)-AngII, even though (Sar_1,Ile_8)-AngII has an association constant several-fold greater than AngII ($K_A = 1.0$–3.3×19^9 M for ^{125}I-(Sar_1,Ile_8)-AngII, depending on its specific activity). The dissociation constant (K_d) values measured in our assay were estimated using a homologous displacement curve method [40]. As summarized in Fig. 6, the K_d for (Sar_1,Ile_8)-AngII was estimated at 3.6×10^{-9} M, which is in good agreement with the expected value of 9.5×10^{-9} M for this batch of ^{125}I-(Sar_1,Ile_8)-AngII. The K_d for the $sc(Fv)_2$-AngII fusion construct was 1.13×10^{-6} M and was comparable to the unmodified AngII (9.4×10^{-5} M).

To further examine the functional effect of $sc(Fv)_2$-AngII on isolated blood vessels in vitro, we conducted a dose–response to $sc(Fv)_2$-AngII in the rat aortic artery and compared the functional effect with norepinephrine (NE). The aortic artery was removed and arterial rings of 3 mm in length were challenged with NE, $sc(Fv)_2$-AngII, and $sc(Fv)_2$, and the vascular contraction was recorded. The functionality of the isolated aortic arteries and the maximum contraction that defined 100% were obtained by the challenge with 5 μM NE. A complete dose–response curve to NE as the standard curve, followed by a complete dose–response curve to $sc(Fv)_2$-AngII, was constructed and the data were calculated as the percent maximum response to NE. The $sc(Fv)_2$-AngII produced an arterial contraction in a dose-dependent fashion of about $16 \pm 1\%$ of the maximum response to

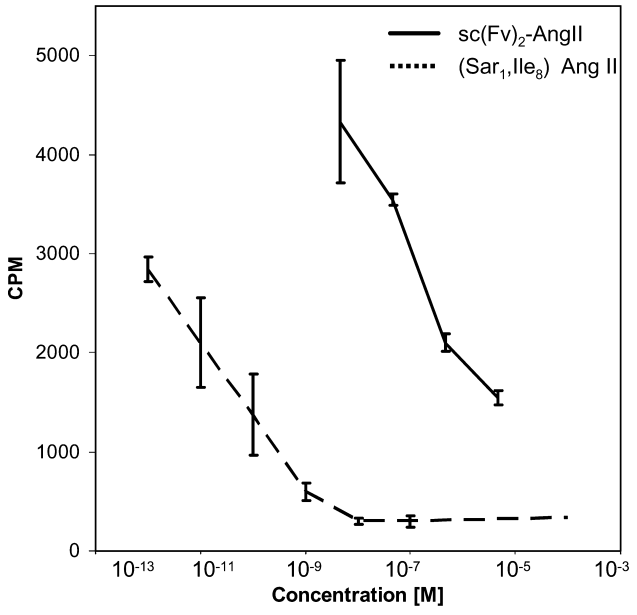

Fig. 6. Binding of the $sc(Fv)_2$-AngII fusion construct to human AT_1 receptor. Increasing amounts of cold (Sar_1,Ile_8)-AngII and $sc(Fv)_2$-AngII were allowed to compete with ^{125}I-(Sar_1,Ile_8)-AngII (specific activity of 2200 Ci/mmol) for binding to membrane bound recombinant human AT_1 receptor. The samples were harvested on GF/C filters, measured in the γ-counter, and the bound counts were plotted against the concentration of the competitor used.

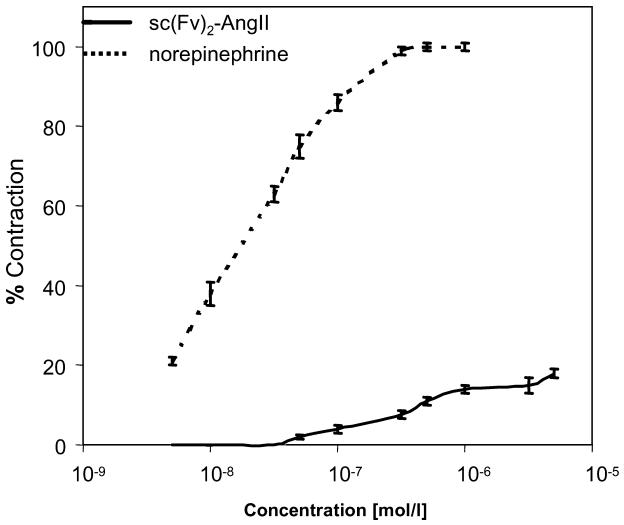

Fig. 7. In isolated tissue bath studies of the contraction of rat aortic artery by the $sc(Fv)_2$-AngII construct, the $sc(Fv)_2$-AngII produced a contraction in a dose-dependent fashion. At the maximum dose of 5 μM, the contraction was $16 \pm 1\%$ of the maximum response to norepinephrine.

5 μM NE (Fig. 7). As in the receptor binding studies, there was no functional effect of the $sc(Fv)_2$ at concentrations similar to the ones used for $sc(Fv)_2$-AngII (data not shown).

In vivo tumor uptake and tumor penetration

The biological effect of the addition of the angiotensin II sequence in the C-terminal end of the $sc(Fv)_2$ was assessed by the bio-distribution in tumor-bearing nude mice (Fig. 8). At a low dose, the %ID in the blood indicated a similar pharmacokinetic pattern of $sc(Fv)_2$-AngII in comparison to $sc(Fv)_2$. Also the relative tumor uptake was not increased with a protein concentration of approximately 0.25 mg/kg bwt. The comparison between $sc(Fv)_2$-AngII and $sc(Fv)_2$ revealed no significant differences in the antibody uptake in the healthy organs. The macroautoradiography, however, showed a more

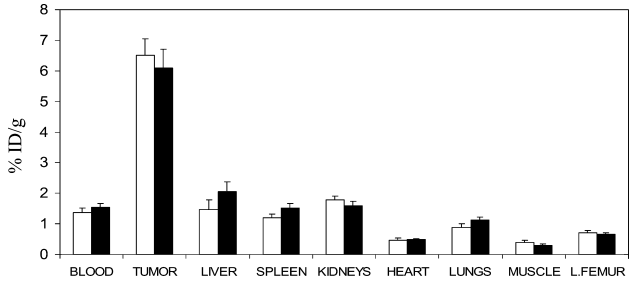

Fig. 8. In vivo biodistribution of radiolabeled $sc(Fv)_2$-AngII and $sc(Fv)_2$-AngII constructs I tumor bearing animals. The tumor uptake of both ^{125}I-labeled constructs was similar and no significant alterations between distribution of $sc(Fv)_2$-AngII and $sc(Fv)_2$construct in normal tissues were observed.

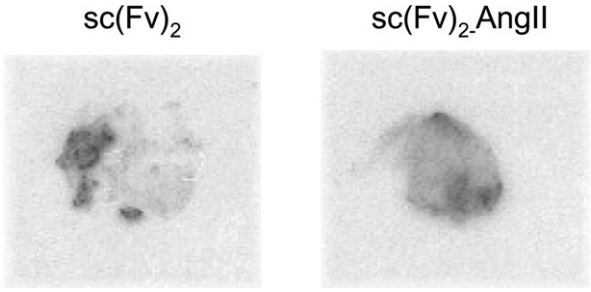

Fig. 9. Macro-autoradiography of the tumors obtained 4 h after the treatment with $sc(Fv)_2$-AngII or $sc(Fv)_2$. Treatment with $sc(Fv)_2$-AngII resulted in a more homogeneous distribution of the radioactivity in comparison to the $sc(Fv)_2$ construct in spite of an unaltered %ID of the actual tumor tissue.

homogeneous distribution of the radiolabeled $sc(Fv)_2$-AngII in the tumor tissue. The tumor uptake of the $sc(Fv)_2$ showed a less homogeneous pattern, with areas of extremely high and areas of a lower uptake of ^{125}I-$sc(Fv)_2$ (Fig. 9).

Discussion

By adding the octapeptide sequence of angiotensin II to the C-terminal end of the $sc(Fv)_2$ molecule, we generated a divalent construct directed against TAG-72 with intrinsic activity to modulate blood flow in the tumor vessels, for the first time. To achieve this, we moved the HisTag required for IMAC to the N-terminal end of the molecule (Fig. 1). These alterations of the $sc(Fv)_2$ molecule did not affect the antigen binding of the $sc(Fv)_2$-AngII fusion construct to BSM (Fig. 2). This was a critical observation, since scFvs can lose their binding affinity, especially when modified at the C-terminus. In the case of the monovalent scFv directed against TAG-72, the placement of the hexahistidine tag on the C-terminal end led to a partial loss in antigen binding affinity. Molecular modeling suggested this to be due to a partial covering of the antigen recognition site [41].

Even though an interference of the antigen binding was not observed with the additional sequences, an interference resulting in a 50% loss of receptor binding to AT_1 receptors occurred, when the angiotensin II sequence was added to the $sc(Fv)_2$ sequence without the 5 AA spacer (data not shown). After the introduction of the amino acid spacer, the AT_1 receptor binding affinity of the CC49 $sc(Fv)_2$-AngII fusion construct was determined to be 1.13×10^{-6} M, a value similar to native angiotensin II, reported to be 9.4×10^{-5} M (Fig. 6). When isolated rat aortic artery was exposed to $sc(Fv)_2$-AngII, the construct also demonstrated its ability to contract arterial vessels in a dose-dependent fashion.

In in vivo tumor localization studies, however, low doses of the fusion construct of approximately 2.5×10^{-9} M/kg BWT did not lead to an increase in tumor uptake (Fig. 8). Even at these low doses, the distribution of the radiolabeled fusion construct seemed to be more homogeneous, in comparison to the control sc(Fv)$_2$ (Fig. 9). This characteristic of angiotensin was observed earlier by Kinuya et al. [28], who reported a more homogeneous distribution, even of the larger IgG, by the combination of angiotensin II and enalapril, an angiotensin-converting enzyme inhibitor. That study indicated that the application of ^{125}I-labeled A7 antibody led to large areas of tumors with almost no uptake in radioactivity in LS-180 colon cancer xenograft tumors. By co-treatment with angiotensin and enalapril, the distribution was far more homogeneous [28].

Another factor greatly influencing the function of angiotensin II in tumor therapy is the tumor mass, which in our model was approximately 200 mg/tumor. In order for angiotensin II to divert the blood flow from healthy tissues with contracted vessels to the neoplasm with vessels incapable of contraction, the tumor has to exceed the size, which requires a neo-vascularization. Consequently, the effect of angiotensin II to increase the tumor blood flow would be, especially in experimental models, more pronounced in larger tumors. The effects of angiotensin on the tumor perfusion in the experimental setting are somewhat contradictory. Some investigators report a clear increase in tumor blood flow, while others show variable effects, or even a reduction in tumor blood flow [24,42–44]. These reports indicate that not only the actual tumor size influences the tumor blood flow, but also further, yet undefined, factors, like tumor type and tumor location, seem to influence the effect of angiotensin II.

Clinically, however, several types of tumors respond well to angiotensin chemotherapy combinations [26]. Especially, in pancreatic cancer, a tumor type almost refractive to radio-, and systemic chemotherapy, the combination of angiotensin II, methotrexate, and 5-fluorouracil applied over an intra-arterial port led to an increase in survival of 16 ± 9 months [45]. Imaging studies, applying angiotensin II via an intra-arterial catheter in pancreatic cancer patients, show that the increase in tumor perfusion is likely explanation for the observed benefit of the therapeutic regimen [46]. These studies indicate that pancreatic cancer patients, with their poor prognosis, might be a patient collective that might benefit from the sc(Fv)$_2$-AngII fusion construct in immunotherapy. In the therapeutic study, however, angiotensin II was administered along with the chemotherapeutic drugs on a biweekly schedule [45]. This, on the other hand, led to a repeated angiotensin II application that can lead, as was shown in rats, to an increase in tumor vascularization [47]. Clinically, this effect was even observed on an individual basis, where a correlation between the vascular densities and the success of the intra-arterial chemotherapy has been established in cervical cancer patients [48]. In terms of the long-term effects of angiotensin II, sc(Fv)$_2$-AngII construct is characterized by a dramatically longer half-life than native angiotensin II and, furthermore, displays improved tumor localization due to its antigen specificity. Especially in the context of the long-term effects of angiotensin II, the sc(Fv)$_2$-AngII might substitute a drug capable of inducing these long-term effects of angiotensin II.

In conclusion, by the addition of the angiotensin sequence to the sc(Fv), we generated a vasoactive molecule that not only has the potential to increase the tumor perfusion on a short-term basis, but also could be used in a long-term therapeutic regimen to possibly alter the angiogenesis in neoplastic tissues. The sc(Fv)$_2$-AngII not only has the potential for immediate, but also long-term, effects, laying the way for chemo- or antibody-based therapeutics. Further pre-clinical studies utilizing our sc(Fv)$_2$-AngII fusion construct, addressing the short- and long-term capabilities, will be performed to develop regimens for improved tumor perfusion.

Acknowledgments

We thank Ms. Kay Devish, Mr. Jason Jokerst, and Mr. Erik Moore for expert technical assistance. We acknowledge the Molecular Biology Core Lab for sequencing studies, the Molecular Interaction Facility for BIAcore studies, and Ms. Kristi L.W. Berger for editorial assistance. The monovalent CC49 scFv construct was a generous gift from the National Cancer Institute Laboratory of Tumor Immunology and Biology (Dr. Schlom) and the Dow Chemical Company.

References

[1] G.R. Thrush, L.R. Lark, B.C. Clinchy, E.S. Vitetta, Immunotoxins: An update, Annu. Rev. Immunol. 14 (1996) 49–71.
[2] H. Zhang, S. Zhang, N.K. Cheung, G. Ragupathi, P.O. Livingston, Antibodies against GD2 ganglioside can eradicate syngeneic cancer micrometastases, Cancer Res. 58 (1998) 2844–2849.
[3] S.K. Imam, Status of radioimmunotherapy in the new millennium, Cancer Biother. Radiopharm. 16 (2001) 237–256.
[4] B. Rippe, B. Haraldsson, Transport of macromolecules across microvascular walls: The two-pore theory, Physiol. Rev. 74 (1994) 163–219.
[5] M.F. Flessner, R.L. Dedrick, Monoclonal antibody delivery to intraperitoneal tumors in rats: Effects of route of administration and intraperitoneal solution osmolality, Cancer Res. 54 (1994) 4376–4384.
[6] P.A. Netti, S. Roberge, Y. Boucher, L.T. Baxter, R.K. Jain, Effect of transvascular fluid exchange on pressure–flow relationship in tumors: A proposed mechanism for tumor blood flow heterogeneity, Microvasc. Res. 52 (1996) 27–46.
[7] T.P. Padera, A. Kadambi, E. di Tomaso, C.M. Carreira, E.B. Brown, Y. Boucher, N.C. Choi, D. Mathisen, J. Wain, E.J.

Mark, L.L. Munn, R.K. Jain, Lymphatic metastasis in the absence of functional intratumor lymphatics, Science 296 (2002) 1883–1886.
[8] R.K. Jain, Barriers to drug delivery in solid tumors, Sci. Am. 271 (1994) 58–65.
[9] R.K. Jain, L.L. Munn, D. Fukumura, Dissecting tumour pathophysiology using intravital microscopy, Nat. Rev. Cancer 2 (2002) 266–276.
[10] P. Carmeliet, R.K. Jain, Angiogenesis in cancer and other diseases, Nature 407 (2000) 249–257.
[11] J.R. Less, M.C. Posner, Y. Boucher, D. Borochovitz, N. Wolmark, R.K. Jain, Interstitial hypertension in human breast and colorectal tumors, Cancer Res. 52 (1992) 6371–6374.
[12] R.K. Jain, L.T. Baxter, Mechanisms of heterogeneous distribution of monoclonal antibodies and other macromolecules in tumors: Significance of elevated interstitial pressure, Cancer Res. 48 (1988) 7022–7032.
[13] Y. Boucher, R.K. Jain, Microvascular pressure is the principal driving force for interstitial hypertension in solid tumors: Implications for vascular collapse, Cancer Res. 52 (1992) 5110–5114.
[14] M. Suzuki, K. Hori, I. Abe, S. Saito, H. Sato, Functional characterization of the microcirculation in tumors, Cancer Metastasis Rev. 3 (1984) 115–126.
[15] N.V. Krylova, Characteristics of microcirculation in experimental tumours, Bibl. Anat. 10 (1969) 301–303.
[16] M. Suzuki, K. Hori, I. Abe, S. Saito, H. Sato, A new approach to cancer chemotherapy: Selective enhancement of tumor blood flow with angiotensin II, J. Natl. Cancer Inst. 67 (1981) 663–669.
[17] M. Kohzuki, S. Tanda, K. Hori, K. Yoshida, M. Kamimoto, X.M. Wu, T. Sato, Endothelin receptors and angiotensin II receptors in tumor tissue, J. Cardiovasc. Pharmacol. 31 (Suppl. 1) (1998) S531–S533.
[18] M.A. Burton, B.N. Gray, G.W. Self, J.C. Heggie, P.S. Townsend, Manipulation of experimental rat and rabbit liver tumor blood flow with angiotensin II, Cancer Res. 45 (1985) 5390–5393.
[19] D.J. Kerr, J.A. Goldberg, J.R. Anderson, N. Wilmott, A.T. Whatelely, C.S. McArdle, J. Mckillop, The effect of angiotensin II on tumor blood flow and the delivery of microparticulate cytotoxic drugs, EXS 61 (1992) 339–345.
[20] N. Mitsuhata, M. Seki, Y. Matsumura, H. Ohmori, Intra-arterial infusion chemotherapy in combination with angiotensin II for advanced bladder cancer, J. Urol. 136 (1986) 580–585.
[21] H. Taniguchi, H. Koyama, M. Masuyama, A. Takada, T. Mugitani, H. Tanaka, M. Hoshima, T. Takahashi, Angiotensin-II-induced hypertension chemotherapy: Evaluation of hepatic blood flow with oxygen-15 PET, J. Nucl. Med. 37 (1996) 1522–1523.
[22] S. Noguchi, K. Miyauchi, Y. Nishizawa, Y. Sasaki, S. Imaoka, T. Iwanaga, H. Koyama, T. Terasawa, Augmentation of anticancer effect with angiotensin II in intraarterial infusion chemotherapy for breast carcinoma, Cancer 62 (1988) 467–473.
[23] D.M. Hemingway, T.G. Cooke, D. Chang, S.J. Grime, S.A. Jenkins, The effects of intra-arterial vasoconstrictors on the distribution of a radiolabelled low molecular weight marker in an experimental model of liver tumour, Br. J. Cancer 63 (1991) 495–498.
[24] K. Tokuda, H. Abe, T. Aida, S. Sugimoto, S. Kaneko, Modification of tumor blood flow and enhancement of therapeutic effect of ACNU on experimental rat gliomas with angiotensin II, J. Neurooncol. 8 (1990) 205–212.
[25] M.A. Burton, B.N. Gray, A. Coletti, Effect of angiotensin II on blood flow in the transplanted sheep squamous cell carcinoma, Eur. J. Cancer Clin. Oncol. 24 (1988) 1373–1376.
[26] H. Sato, K. Sugiyama, M. Hoshi, M. Urushiyama, K. Ishizuka, Angiotensin II (AII) induced hypertension chemotherapy (IHC) for unresectable gastric cancer: With reference to resection after down staging, World J. Surg. 19 (1995) 836–842.
[27] A. Takeda, T. Miyoshi, H. Shimada, T. Ochiai, K. Isono, Enhanced effects of monoclonal antibody carboplatin immunoconjugates uptake and anti-tumor effects with angiotensin II and tumor necrosis factor, J. Chemother. 11 (1999) 137–143.
[28] S. Kinuya, K. Yokoyama, A. Kawashima, T. Hiramatsu, S. Konishi, N. Shuke, N. Watanabe, T. Takayama, T. Michigishi, N. Tonami, Pharmacologic intervention with angiotensin II and kininase inhibitor enhanced efficacy of radioimmunotherapy in human colon cancer xenografts, J. Nucl. Med. 41 (2000) 1244–1249.
[29] I. Abe, K. Hori, S. Saito, S. Tanda, Y.L. Li, M. Suzuki, Increased intratumor concentration of fluorescein-isothiocyanate-labeled neocarzinostatin in rats under angiotensin-induced hypertension, Jpn. J. Cancer Res. 79 (1988) 874–879.
[30] J.A. Goldberg, M.S. Bradnam, D.J. Kerr, J.H. McKillop, R.G. Bessent, C.S. McArdle, N. Willmott, W.D. George, Single photon emission computed tomographic studies (SPECT) of hepatic arterial perfusion scintigraphy (HAPS) in patients with colorectal liver metastases: Improved tumour targetting by microspheres with angiotensin II, Nucl. Med. Commun. 8 (1987) 1025–1032.
[31] A. Goel, D. Colcher, J. Baranowska-Kortylewicz, S. Augustine, B.J. Booth, G. Pavlinkova, S.K. Batra, Genetically engineered tetravalent single-chain Fv of the pancarcinoma monoclonal antibody CC49: Improved biodistribution and potential for therapeutic application, Cancer Res. 60 (2000) 6964–6971.
[32] A. Goel, G.W. Beresford, D. Colcher, G. Pavlinkova, B.J. Booth, J. Baranowska-Kortylewicz, S.K. Batra, Divalent forms of CC49 single-chain antibody constructs in *Pichia pastoris*: Expression, purification, and characterization, J. Biochem. 127 (2000) 829–836.
[33] A. Goel, S. Augustine, J. Baranowska-Kortylewicz, D. Colcher, B.J. Booth, G. Pavlinkova, M. Tempero, S.K. Batra, Single-dose versus fractionated radioimmunotherapy of human colon carcinoma xenografts using 131I-labeled multivalent CC49 single-chain fvs, Clin. Cancer Res. 7 (2001) 175–184.
[34] D. Colcher, A. Goel, G. Pavlinkova, G. Beresford, B. Booth, S.K. Batra, Effects of genetic engineering on the pharmacokinetics of antibodies, Q. J. Nucl. Med. 43 (1999) 132–139.
[35] G. Pavlinkova, G.W. Beresford, B.J. Booth, S.K. Batra, D. Colcher, Pharmacokinetics and biodistribution of engineered single-chain antibody constructs of MAb CC49 in colon carcinoma xenografts, J. Nucl. Med. 40 (1999) 1536–1546.
[36] D. Colcher, G. Pavlinkova, G. Beresford, B.J. Booth, A. Choudhury, S.K. Batra, Pharmacokinetics and biodistribution of genetically-engineered antibodies, Q. J. Nucl. Med. 42 (1998) 225–241.
[37] G. Pavlinkova, G. Beresford, B.J. Booth, S.K. Batra, D. Colcher, Charge-modified single chain antibody constructs of monoclonal antibody CC49: Generation, characterization, pharmacokinetics, and biodistribution analysis, Nucl. Med. Biol. 26 (1999) 27–34.
[38] D. Colcher, M. Zalutsky, W. Kaplan, D. Kufe, F. Austin, J. Schlom, Radiolocalization of human mammary tumors in athymic mice by a monoclonal antibody, Cancer Res. 43 (1983) 736–742.
[39] D. Colcher, R. Bird, M. Roselli, K.D. Hardman, S. Johnson, S. Pope, S.W. Dodd, M.W. Pantoliano, D.E. Milenic, J. Schlom, In vivo tumor targeting of a recombinant single-chain antigen-binding protein, J. Natl. Cancer Inst. 82 (1990) 1191–1197.
[40] A. Larsson, B. Axelsson, Calculation of affinity constants directly from homologous displacement curves, J. Immunol. Methods 137 (1991) 253–259.
[41] A. Goel, D. Colcher, J.S. Koo, B.J. Booth, G. Pavlinkova, S.K. Batra, Relative position of the hexahistidine tag effects binding properties of a tumor-associated single-chain Fv construct, Biochim. Biophys. Acta 1523 (2000) 13–20.
[42] N. Tomura, T. Kato, I. Kanno, F. Shishido, A. Inugami, K. Uemura, S. Higano, H. Fujita, K. Mineura, M. Kowada,

Increased blood flow in human brain tumor after administration of angiotensin II: Demonstration by PET, Comput. Med. Imaging Graph. 17 (1993) 443–449.
[43] R.A. Zlotecki, Y. Boucher, I. Lee, L.T. Baxter, R.K. Jain, Effect of angiotensin II induced hypertension on tumor blood flow and interstitial fluid pressure, Cancer Res. 53 (1993) 2466–2468.
[44] G.M. Tozer, K.M. Shaffi, Modification of tumour blood flow using the hypertensive agent, angiotensin II, Br. J. Cancer 67 (1993) 981–988.
[45] H. Ohigashi, O. Ishikawa, S. Imaoka, Y. Sasaki, T. Kabuto, M. Kameyama, H. Furukawa, M. Hiratuka, S. Nakamori, H. Nakano, T. Yasuda, T. Iwanaga, A new method of intra-arterial regional chemotherapy with more selective drug delivery for locally advanced pancreatic cancer, Hepatogastroenterology 43 (1996) 338–345.
[46] C. Kuroda, N. Mihara, N. Hosomi, E. Inoue, M. Fujita, H. Ohigashi, O. Ishikawa, A. Nakaizumi, S. Ishiguro, Spiral CT during pharmacoangiography with angiotensin II in patients with pancreatic disease. Technique and diagnostic efficacy, Acta Radiol. 39 (1998) 138–143.
[47] K. Hori, M. Suzuki, I. Abe, S. Saito, H. Sato, Increase in tumor vascular area due to increased blood flow by angiotensin II in rats, J. Natl. Cancer Inst. 74 (1985) 453–459.
[48] Y. Kohno, O. Iwanari, M. Kitao, Prognostic importance of histologic vascular density in cervical cancer treated with hypertensive intraarterial chemotherapy, Cancer 72 (1993) 2394–2400.